The Astrophysical Journal, 785:22 (5pp), 2014 April 10 doi:10.1088/0004-637X/785/1/22

HYDROGEN FLUORIDE TOWARD LUMINOUS NEARBY GALAXIES: NGC 253 AND NGC 4945

R. R. Monje[1], S. Lord[2], E. Falgarone[3], D. C. Lis[1], D. A. Neufeld[4], T. G. Phillips[1], and R. Güsten[5]
[1] California Institute of Technology, 1200 East California Boulevard, Pasadena, CA 91125-4700, USA; raquel@caltech.edu
[2] Infrared Processing and Analysis Center, California Institute of Technology, MS 100-22, Pasadena, CA 91125, USA
[3] LERMA/LRA, Ecole Normale Supérieure & Observatoire de Paris, 24 rue Lhomond, F-75005 Paris, France
[4] Department of Physics and Astronomy, Johns Hopkins University, 3400 North Charles Street, Baltimore, MD 21218, USA
[5] Max-Planck Institut für Radioastronomie, Auf dem Hügel 69, D-53121 Bonn, Germany
Received 2013 October 1; accepted 2014 February 11; published 2014 March 21

ABSTRACT

We present the detection of hydrogen fluoride (HF) in two luminous nearby galaxies, NGC 253 and NGC 4945 using the Heterodyne Instrument for the Far-Infrared on board the *Herschel Space Observatory*. The HF line toward NGC 253 has a P-Cygni profile, while an asymmetric absorption profile is seen toward NGC 4945. The P-Cygni profile in NGC 253 suggests an outflow of molecular gas with a mass of $M(H_2)_{out} \sim 1 \times 10^7\ M_\odot$ and an outflow rate as large as $\dot{M} \sim 6.4\ M_\odot\ yr^{-1}$. In the case of NGC 4945, the axisymmetric velocity components in the HF line profile are compatible with the interpretation of a fast-rotating nuclear ring surrounding the nucleus and the presence of inflowing gas. The gas falls into the nucleus with an inflow rate of $\leqslant 1.2\ M_\odot\ yr^{-1}$, inside an inner radius of $\leqslant 200$ pc. The gas accretion rate to the central active galactic nucleus is much smaller, suggesting that the inflow may be triggering a nuclear starburst. From these results, the HF $J = 1$–0 line is seen to provide an important probe of the kinematics of absorbing material along the sight-line to nearby galaxies with bright dust continuum and a promising new tracer of molecular gas in high-redshift galaxies.

Key words: astrochemistry – submillimeter: ISM – ISM: abundances – ISM: molecules

Online-only material: color figures

1. INTRODUCTION

Herschel Space Observatory (Pilbratt et al. 2010), and in particular its Heterodyne Instrument for Far-Infrared (HIFI; de Graauw 2010) has facilitated observations at high-spectral resolution of interstellar hydride molecules—compounds with one or more hydrogen and one heavy element atom—in the local universe ($z \sim 0$). Most of the hydride molecule observations are inaccessible from ground-based telescopes because their high frequency rotational transitions are blocked by the large opacity of Earth's atmosphere. Two key results from *Herschel*/HIFI were the first detection of the *fundamental* $J = 1$–0 rotational transition of hydrogen fluoride (HF) at 1.232 THz (243 μm) and the discovery of HF's ubiquitous nature in the Milky Way. HF has not only been observed in almost every bright continuum source in the Galactic plane (Phillips et al. 2010; Sonnentrucker et al. 2010; Neufeld et al. 2010; Monje et al. 2011a), but also in some nearby ultra-luminous galaxies (van der Werf et al. 2010; Rangwala et al. 2011), establishing its importance outside the Milky Way as well. Despite fluorine's (F) relative low abundance in the interstellar medium (ISM; about four times lower than carbon), F plays an important role in the interstellar chemistry due to the unique thermochemistry of the reaction between F and molecular hydrogen (H_2). F is the only atom that reacts exothermically with H_2, to form the compound HF. Once formed, HF becomes the main reservoir of fluorine in the ISM, with a strong bond only destroyed by reactions with low abundance ions H_3^+, C^+, and He^+, or photodissociation, with an estimated photodissociation rate of $1.17 \times 10^{-10}\ s^{-1}$. This unusual stability allows the buildup of large amounts of HF in the ISM, which has now been confirmed by *Herschel*.

Theoretical models from Neufeld et al. (2005) originally predicted that the HF abundance in diffuse clouds of small extinction ($A_V < 0.5$), could be larger than that of the carbon monoxide (CO)—the main tracer of molecular hydrogen in the submillimeter range—despite the lower abundance of gas-phase fluorine compared to that of carbon. Furthermore, the models also showed that HF may be a more reliable tracer of H_2 than CO, since it presents a constant HF/H_2 ratio (see Figure 6 in Neufeld et al. 2005) with respect to the total visual extinction through the cloud, while the CO/H_2 ratio decreases in clouds of small A_V.

Thus, the Neufeld et al. (2005) model predicted that the ground state rotational transition line of HF $J = 1$–0 would yield an extremely sensitive probe of the diffuse molecular gas along the line of sight to background far-infrared continuum sources and a potential valuable surrogate for molecular hydrogen. The high Einstein coefficient for the spontaneous emission coefficient of the HF $J = 1$–0 line, $A_{10} = 2.42 \times 10^{-2}\ s^{-1}$, results in simple excitation with very high critical density ($\sim 10^9\ cm^{-3}$) at which collisional processes become important for the excitation. Thus, under typical conditions characteristic of the diffuse or even dense ISM, the HF molecules are mainly in the ground rotational state. As a result of its large A_{10} coefficient, the HF $J = 1$–0 line has also been observed primarily in absorption. Only an extremely dense region or a strong radiation field could generate enough excitation to yield an HF feature with a positive frequency-integrated flux. van der Tak et al. (2012) present HF observations toward the Orion Bar, where the line appears in emission. They demonstrate that the excitation of HF is dominated by collisions with electrons and argue that similar conditions can be found toward active galaxies such as Mrk 231 (van der Werf et al. 2010), where the radiation field is strong and the HF line also appears in emission.

The HIFI observations support the theoretical predictions that HF will be the dominant reservoir of interstellar fluorine *under a wide range of conditions*. The most interesting aspect is that HF will likely be an important tracer of molecular gas in high-redshift galaxies, as seen by recent observations with the Caltech Submillimeter Observatory that revealed the highest-redshift

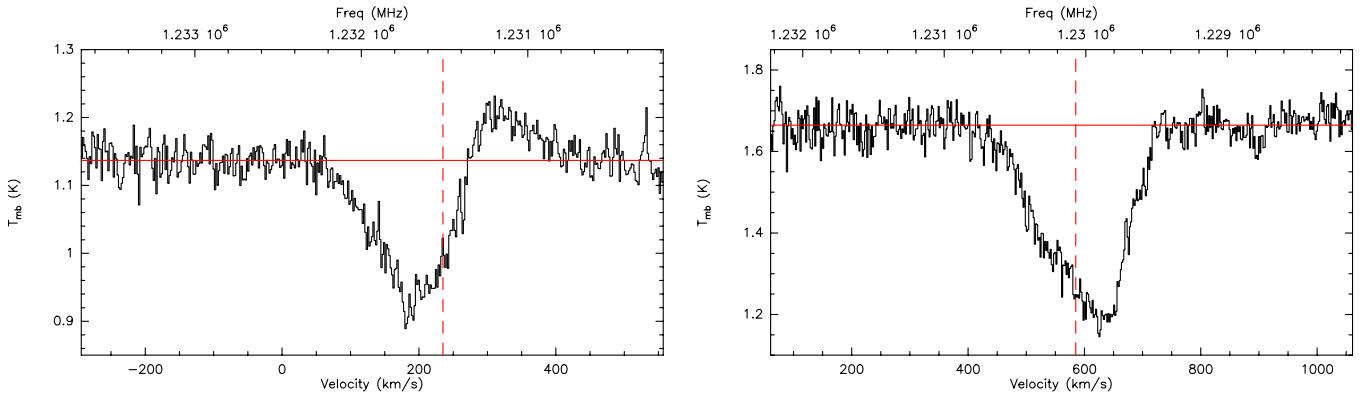

Figure 1. Spectra of the $J = 1$–0 transition of HF toward NGC 253 (left) and NGC 4945 (right). The velocity scale on the lower axis is with respect to the HF $J = 1$–0 rest frequency (1232.4762 GHz). Upper axis shows the frequency scale in MHz. The vertical dashed line corresponds to the systemic $v_{\rm SYS}$, the horizontal solid line shows a zeroth order baseline.

(A color version of this figure is available in the online journal.)

detection of interstellar HF to date toward the luminous lensed Cloverleaf galaxy at $z = 2.558$ (Monje et al. 2011b). High-redshift HF observations will be done routinely with the large collecting area of the Atacama Large Millimeter/submillimeter Array. However, to qualitatively analyze the distant galaxy measurements, a good understanding of HF in the galaxies in the local universe is needed, which, to date, is only achievable with *Herschel*. In this paper, we study the HF content of two nearby galaxies NGC 253 and NGC 4945, prototypical examples of a nearby starburst, and a composite active galactic nucleus (AGN)—starburst nuclei, respectively. NGC 253 is an edge-on ($i = 78°$), nearby, barred galaxy associated with the Sculptor group at a distance of $D = 3.5$ Mpc, with an IR luminosity of $L_{\rm FIR} = 1.7 \times 10^{10} L_{\odot}$ (Radovich et al. 2001) that originated in intense massive star formation regions within its central few hundred parsecs (Strickland et al. 2004). It is also suggested that NGC 253 contains a weak AGN in conjunction with the strong starburst (e.g., Müller-Sánchez et al. 2010). NGC 4945 is also a nearly edge-on ($i = 78°$) local galaxy, part of the Centaurus group at a distance of ∼3.8 Mpc (Karachentsev et al. 2007), with a total infrared luminosity of $L_{\rm FIR} = 2.4 \times 10^{10} L_{\odot}$ (Brock et al. 1988).

In Sections 2 and 3, the observations and results are described. In Section 3.1, we obtain the HF column density for each galaxy. Outflow and inflow gas properties and their nature are discussed in Sections 3.2 and 3.3, and conclusions in are presented Section 4.

2. OBSERVATIONS

Using the *Herschel*/HIFI band 5a receiver, we observe the $J = 1$–0 line of HF toward NGC 253 ($\alpha_{J2000} = 00^{\rm h}47^{\rm m}33\overset{\rm s}{.}1$ and $\delta_{\rm J2000} = -15°17'17\overset{''}{.}6$) and NGC 4945 ($\alpha_{J2000} = 13^{\rm h}05^{\rm m}27\overset{\rm s}{.}48$ and $\delta_{\rm J2000} = -49°28'05\overset{''}{.}6$). The rest frequency of the line is 1232.4762 GHz (Nolt et al. 1987). The NGC 253 data was observed as part of the OT2 (Open Time 2) proposal: *Hydrogen Fluoride Absorption Toward Luminous Infrared Galaxies* (PI: S. Lord), while the NGC 4945 data was obtained as part of the *Herschel* EXtraGALactic key project (PI: R. Güsten). Observations were made using the dual beam switch mode with reference beams located at PA 260 and 296 degrees for NGC 253 and NGC 4945, respectively. We used the HIFI Wide Band Spectrometer, providing a spectral resolution of 1.1 MHz, corresponding to a velocity resolution of 0.27 km s^{-1} at the frequency of $J = 1$–0 line, over a 4 GHz IF bandwidth. The observations of HF toward NGC 253 were obtained using three nearly adjacent local oscillator settings that were averaged to produce the final spectra.

The initial data reduction was carried out using the *Herschel* interactive processing environment (Ott 2010) with pipeline version 9. The IRAM GILDAS package[6] was then used to average the individual spectra scans and for the subsequent data analysis. The HIFI beam size at the line frequency is 17″ with assumed main beam efficiency ($\eta_{\rm mb}$) of 0.64 (Roelfsema et al. 2012). The resultant spectra present a double side band (DSB) continuum main beam temperature of 1.14 and 1.66 K, and an rms noise of 22 and 36 mK at a velocity resolution of 2 km s^{-1} toward NGC 253 and NGC 4945, respectively. The data quality is excellent as shown in Figure 1, where a zeroth order baseline is indicated with the horizontal solid line.

3. RESULTS

Figure 1 shows the HF $J = 1$–0 line observed toward the nuclei of NGC 253 and NGC 4945. The line spectrum toward NGC 253 shows blue shifted absorption and redshifted emission, i.e., a P-Cygni profile. The high resolution absorption HF line spectrum toward NGC 253 covers a velocity range of about ∼80–283 km s^{-1}, and reveals a shift in velocity with respect to the central velocity. The absorption feature is centered at ∼196 km s^{-1}, a much lower velocity than the systemic velocity, 235 km s^{-1} marked with the dashed line in Figure 1, with the deepest absorption feature even further blue shifted. The HF spectrum is very similar to the H I absorption profile (Figure 2) observed toward the nucleus of NGC 253 (Koribalski et al. 1995) and several OH spectral lines (Turner et al. 1985; Bradford et al. 1999; Sturm et al. 2011) covering a similar velocity range to the HF absorption line and also showing an equivalent velocity shift.

The HF spectrum toward NGC 4945 shows an asymmetric absorption profile, with at least two velocity components, in the velocity range of ∼460–715 km s^{-1}. To isolate each individual velocity component and obtain the corresponding line width and center velocity, we fit the spectrum with two Gaussian components centered at ∼540 and 640 km s^{-1} (see Figure 3). These two absorption features are also observed in the H I absorption spectrum as shown in Figure 3.

[6] http://www.iram.fr/IRAMFR/GILDAS/

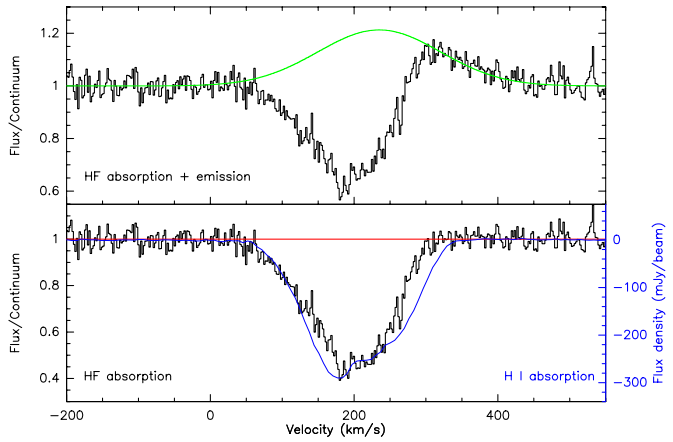

Figure 2. Upper panel: spectrum of the ground-state transition of HF $J = 1$–0 (black) normalized by the corresponding continuum toward NGC 253 and the Gaussian fit (green) of the emission component. Lower panel: HF normalized absorption profile (black) obtained after subtracting the Gaussian line. H I absorption spectrum (blue, in LSR velocities) toward the central continuum source from Koribalski et al. (1995) is also shown for comparison, the conversion between heliocentric velocities and LSR velocities is $v_{\rm LSR} = v_{\rm HSR} - 2.95$ km s^{-1}.

(A color version of this figure is available in the online journal.)

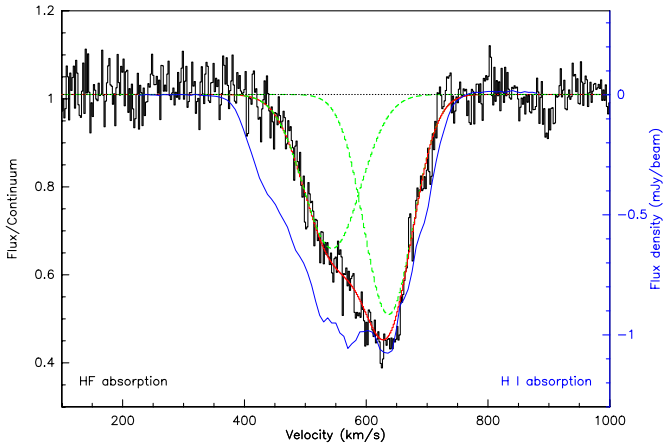

Figure 3. Normalized spectrum of the ground-state transition of HF $J = 1$–0 (black) with respect to the continuum toward NGC 4945 and two Gaussian fits (dashed green lines) center at 543 km s^{-1} and 637 km s^{-1} with δV(FWHM) = 47 km s^{-1} and δV(FWHM) = 40 km s^{-1}, respectively. H I absorption spectrum (blue, in LSR velocities) toward the central continuum source from Ott et al. (2001) is shown for comparison.

(A color version of this figure is available in the online journal.)

3.1. Column Densities of the Absorbing HF Gas

From the line-to-continuum ratio in the absorption profiles we can obtain a direct measurement of the HF column densities. First, we derive apparent optical depths of the HF lines ($\tau = -\ln[2T_{\rm L}/T_{\rm C} - 1]$, where the spectrum is normalized with respect to the single sideband continuum), assuming that the foreground absorption covers the continuum source[7] entirely, and that all HF molecules are in the ground rotational state, due to the large spontaneous emission coefficient of HF and low rates of collisional excitation. The resulting normalized spectra are shown in Figures 2 and 3. For NGC 253, we calculate the optical depth from the absorption profile obtained after subtracting a Gaussian line centered at the systemic velocity, fitting the emission component of the HF spectrum (see Figure 2). The velocity integrated optical depth ($\int \tau d$V) over the velocity interval from 63 to 295 km s^{-1} for NGC 253 and from 445 and 720 km s^{-1} for NGC 4945, is 100 and 115 km s^{-1}, respectively. We thus derive the HF column densities for the correspondent LSR velocity range using Equation (3) of Neufeld et al. (2010) and obtain total HF column densities of $2.41 \pm 0.73 \times 10^{14}$ and $2.77 \pm 0.85 \times 10^{14}$ cm^{-2} toward NGC 253 and NGC 4945, respectively. The uncertainties in the resultant column densities are originated from the random noise and the systematic errors introduced by the calibration uncertainties (Roelfsema et al. 2012)

3.2. Gas Kinematics—Molecular Outflow in NGC 253

A rotating nuclear disk of cold gas in NGC 253 was suggested as a result of the velocity shift of the absorption feature seen in the H I spectrum (Koribalski et al. 1995). In addition to the rotation, the P-Cygni profile present in the HF spectrum line and also in the OH spectra (e.g., Sturm et al. 2011) indicates a radial motion of gas, characteristic of an outflow. The blue-shifted absorption must arise from a region in front of the continuum originating from the nucleus and moving away from it and toward us along the line of sight. The redshifted emission in the HF profile, must then originate from gas behind the continuum source and move away from the nucleus and us. To estimate the molecular mass in the outflow, we adopt an HF abundance relative to H_2 of 3.6×10^{-8}, based on the chemical predictions of Neufeld et al. (2005), consistent also with the HF abundances observed toward galactic diffuse clouds (Sonnentrucker et al. 2010; Monje et al. 2011a) and outflows (e.g., Emprechtinger et al. 2012). In high-mass, star-forming regions, however, where the densities are much higher compare to those of diffuse clouds, the obtained HF abundances are lower by about two orders of magnitude (e.g., Emprechtinger et al. 2012 derived HF abundances as low as 5×10^{-10} in the denser parts of the massive star formation region of NGC 6334 I). The low abundance of HF under these dense (10^5–10^6 cm^{-3}) and warm (100–150 K) conditions is most likely caused by the freeze-out of HF onto dust grains. The polar nature of HF implies large desorption energy. However, dynamically active regions such as outflows and inflows can provide the needed energy for this desorption, and HF abundances in these active regions are similar to those found in diffuse clouds (few 10^{-8}; Emprechtinger et al. 2012). This explanation is supported by evidence for thermal desorption of another polar molecule, H_2O, in dynamically active outflow (Franklin et al. 2008; Kristensen et al. 2010). Thus, using the theoretical HF/H_2 abundance and a source size equal to the beam size 17″ (∼300 pc), the mass[8] of the outflowing gas is $M(H_2)_{\rm out} = 0.97 \times 10^7\ M_\odot$. The outflow projected maximum (terminal) velocity measured from the absorbing gas is about 130 km s^{-1}, measured from the velocity interval, where the absorption is deeper than 3σ ($v_{\rm SYS} - 100$) km s^{-1}. The outflow in NGC 253 has its central axis normal to the galaxy disk (i.e., $i = 12°$; Westmoquette et al. 2011), then the actual maximum outflow velocity is ∼194 km s^{-1}. The outflow extends from a few hundred parsecs to tens of kiloparsecs, with the majority of the molecular gas

[7] The continuum at 180 μm and 350 μm extents to a diameter of ∼10 kpc (Melo et al. 2002) and ∼1.6 kpc (Gear et al. 1986), respectively, much larger than the HIFI beam at the HF wavelength, equivalent to a 0.3 kpc diameter on the source.

[8] The mass is given by $M_{\rm H_2} = m_{\rm H} \times \mu_{\rm H_2} \times N_{\rm H_2} \times D^2 \times \Omega$, where $m_{\rm H}$ is the H-atom mass, $\mu_{\rm H_2} \sim 2.8$ is the molecular weight per hydrogen molecule, D is the distance to the source, and $\Omega = \theta^2\pi/4$ is the solid angle, with θ the angular diameter.

located within a radius of $\leqslant$1 kpc (Young et al. 1995). We assume a compact outflow scenario which extends to 300 pc, the region of intense star-formation activity, and the full extension of the molecular outflow of 1 kpc. Thus, a range of outflow radii from ~300–1000 pc implies a dynamical time of $t_{\rm dyn} = R/V =$ 1.51–5.03 $\times$ 10^6 yr. The resulting molecular mass loss rate is $\delta M/\delta t = \dot{M} =$ 1.93–6.43 $M_\odot$ yr^{-1}. Note that these values are consistent with that obtained using the OH absorption line (Sturm et al. 2011) and the more direct measurements of CO from Bolatto et al. (2013), which imply values of $1.6^{+4.8}_{-1.2}$ and ~3 $M_\odot$ yr^{-1}, respectively. The outflow rate estimates from HF provide a measurement independent of uncertainties introduced by the CO-to-H_2 conversion factor, $\alpha_{\rm CO}$, and even though the derived $\dot{M}$ depends on the adopted HF abundance relative to H_2, lower HF abundances will lead to larger outflow rates.

3.2.1. What Mechanism is Driving the Outflow?

Galactic-scale outflows are common phenomena, detected in most active, star-forming galaxies in the local universe (Colbert et al. 1996) and at high redshifts (Pettini et al. 2001). They are the key mechanism by which energy and metals are recycled in galaxies and deposited into the intergalactic medium. Outflows are thus closely connected with galaxy formation and evolution, potentially regulating the growth of massive galaxies and the thermal properties of the intracluster medium in galaxy groups and clusters (e.g., Silk & Rees 1998). To date, most of the relevant information on outflows has come from observations of X-ray emission produced by the hot gas, the optical line emission produced by the warm gas, and interstellar absorption lines. Molecular outflows have also been detected by means of ^{12}CO and high-density tracers—such as HCN—line wings (e.g., Aalto et al. 2012). The dominant outflow mechanism, whether *starburst-driven*, where the winds are driven by the mechanical energy and momentum from stellar winds and supernovae; or *AGN-driven*, where the black hole activity may also trigger outflows by accretion, is rarely unambiguously determined (see review by Veilleux et al. 2005). In the case of NGC 253, there is extensive observational evidence that points toward the starburst driven outflow scenario in its central region (Strickland et al. 2000; Forbes et al. 2000; Weaver et al. 2002). The line widths can help to determine the nature of the outflow, as described in Sturm et al. (2011), where a coarse correlation between the outflow velocity and $L_{\rm AGN}$ is obtained. Furthermore, studies by Rupke et al. (2005) and Krug et al. (2010) show that ULIRGs with high AGN fractions have high outflow velocities ($\geqslant$1000 km s^{-1}), while the HF absorption line and other molecular lines, such as OH, seen toward NGC 253, present line widths of less than 300 km s^{-1}. Assuming an outflow driven by the wind momentum of massive stars, we estimate the star formation rate (SFR($M_\odot$ yr^{-1}) $\approx L_{\rm IR} \times 10^{-10}$, Kennicutt 1998) of 1.7 $M_\odot$ yr^{-1}, calculated from the IR luminosities (with FIR solely due to star formation). The SFR is comparable to the outflow rates ($\dot{M}$) calculated in the previous section with the HF outflow parameters, when one takes into account the uncertainties in the outflow mass and structure, resulting from the lack of angular resolution to determine the spatial distribution of the outflow material traced by HF. Thus, it appears that the SFR could expel the cold gas by wind-momentum of massive stars. Another interesting mechanism that can drive the outflow is the radiation pressure from the absorption and scattering of starlight by dust grains. The radiation can be produced both by a starburst or an AGN. Murray et al. (2005) suggested that for a radiation pressure driven outflow the total momentum deposition rate ($\dot{P} \approx \dot{M}V$) should be equivalent to the total momentum flux (L/c, where L is the starburst contribution to the total luminosity). For NGC 253, the momentum deposition rate is comparable to the total momentum flux. Therefore, the pressure driven scenario cannot be discarded.

3.3. Gas Kinematics in NGC 4945

The HF observations in NGC 4945 show an absorption feature with at least two components centered at ~540 and 640 km s^{-1}, shown in Figure 3. For comparison, Figure 3 also shows the absorption profile of H I (Ott et al. 2001) observed toward the nucleus. These almost axi-symmetric gas components, at $v_{\rm SYS} \pm$ 50 km s^{-1}, taking $v_{\rm SYS}$ ~ 585 km s^{-1} (Chou et al. 2007), can indicate two possible scenarios, the presence of a nuclear *molecular gas ring* and an *inflowing gas motion*. The existence of rapidly rotating clouds surrounding the nucleus has been suggested previously in studies of several molecular lines, such as OH (Whiteoak & Wilson 1990), CO (Whiteoak et al. 1990), and H I (Ott et al. 2001) line observations, where spatially resolved maps of the nucleus of NGC 4945 support the existence of two concentric fast-rotating nuclear rings surrounding the nucleus within a radius of $\leqslant$200 pc. Simultaneously, Figure 3 shows a prominent HF and H I feature at 640 km s^{-1}, also observed as an absorption dip in the CO spectra (Dahlem et al. 1993), that traces red-shifted foreground gas moving toward the center of the galaxy and can be interpreted as an infall signature. Signatures for inflowing molecular gas at similar velocities have also been found in high-density gas tracers such as, HCN, HCO^+, and CN (Henkel et al. 1990), where an absorption dip is seen in the emission line profiles.

Following the discussion in the previous section, we can estimate the inflowing gas physical properties seen toward NGC 4945. The HF column density of the inflowing gas, i.e., within the velocity interval of 560 to 720 km s^{-1}, is 1.45 $\times$ 10^{14} cm^{-2}. Assuming an HF abundance with respect to H_2 of 3.6 $\times$ 10^{-8} and a source size of 8″ (≈200 pc), the inflow mass is 1.54 $\times$ 10^6 $M_\odot$. Taking 200 pc as an upper limit to the inflow radius and a maximum inflow velocity of 152 km s^{-1},[9] the derived molecular mass loss rate is $\dot{M} \leqslant 1.2\,M_\odot$ yr^{-1}. This relative high inflow rate is ~3 orders of magnitude greater than that needed to power the AGN itself (accretion rate of 0.0031 $M_\odot$ yr^{-1}; Lin et al. 2011). Evidence of starburst in an NGC 4945 region of a few parsecs in size, has been shown by Chou et al. (2007) using the Submillimeter Array, where several molecular lines were observed at an angular resolution of a few arcseconds, tracing an inclined rotating disk with the major axis aligned with that of the stardust ring (a 100 pc diameter ring observed in Paα, Marconi et al. 2000). Therefore, this could be a case where the gas inflow is fueling the nuclear starburst. Similar scenarios of inflow, fueling the central tens of parsecs starburst, have also been reported in analogous galaxies, such as, NGC 1097 (Davies et al. 2009).

4. CONCLUSIONS

We present the detection of the HF J = 1–0 transition in two nearby galaxies, NGC 253 and NGC 4945. The HF spectrum toward NGC 253 shows a P-Cygni profile, with the absorption blue-shifted with respect to the systemic velocity, as expected for

[9] The maximum inflow velocity is estimated using a maximum inflow projected velocity of 134 km s^{-1} with a nuclear inclination of ~62°, Chou et al. (2007), smaller than the inclination of the large-scale galactic disk of ~78°.

an outflow system. Estimated outflow parameters derived from the HF spectrum are mass of the outflowing gas $M(H_2)_{out} \sim 1 \times 10^7\ M_\odot$; the molecular mass loss rate $\dot{M} \leqslant 6.4\ M_\odot\ yr^{-1}$; and a maximum, unprojected outflow velocity of $v_{out} \sim 194$ km s^{-1}. The relatively small outflow velocity and the SFR comparable to the outflow rate, argue for a starburst nature of the outflow, however other driving mechanisms, such as radiation pressure, cannot be ruled out. While the HF spectrum shows clear evidence of a molecular outflow, the conclusions about its nature need further confirmation with spatially resolved observations or a larger statistical sample. The HF line toward NGC 4945 shows an asymmetric absorption feature, where we can distinguish two components at almost axisymmetric velocities with respect to the systemic velocity ($v_{sys} \pm 50$ km s^{-1}). The axisymmetry velocity profile is compatible with the ring and inflowing gas scenarios, where the redshifted component can be interpreted as a signature of gas falling onto the nucleus. The relatively high inflow rate obtained from the absorption spectrum, indicates gas triggering a nuclear starburst. However, higher angular resolution is needed to reach a firmer conclusion about the nuclear kinematics of NGC 4945.

From these results, the HF $J = 1$–0 line promises to provide a valuable probe of the kinematics of absorbing material along the sight line to bright extragalactic continuum sources. HF $J = 1$–0 line observations toward a larger sample of nearby (U)LIRGs, including radiative transfer models will be presented in a future publication. Studies with larger statistical samples will be able to establish a correlation between the HF abundance and the physical conditions, especially density and temperature. The characterization of HF line observations toward nearby galaxies will be an important tool for understand future observations of HF at high redshift, where the HF line could be a relevant probe of molecular gas in dense, but especially in lower density, regions of those high redshifted sources where the redshifted H I frequency falls outside the frequency allocation windows for radio astronomy.

R.M. thanks Nick Scoville for reading through the manuscript and providing very helpful comments. HIFI has been designed and built by a consortium of institutes and university departments from across Europe, Canada, and the United States under the leadership of SRON Netherlands Institute for Space Research, Groningen, The Netherlands, and with major contributions from Germany, France, and the US. Consortium members are, Canada: CSA, University of Waterloo; France: CESR, LAB, LERMA, IRAM; Germany: KOSMA, MPIfR, MPS; Ireland, NUI Maynooth; Italy: ASI, IFSI-INAF, Osservatorio Astrofisico di Arcetri-INAF; Netherlands: SRON, TUD; Poland: CAMK, CBK; Spain: Observatorio Astronomico Nacional (IGN), Centro de Astrobiología (CSIC-INTA). Sweden: Chalmers University of Technology-MC2, RSS & GARD; Onsala Space Observatory; Swedish National Space Board, Stockholm University—Stockholm Observatory; Switzerland: ETH Zurich, FHNW; USA: Caltech, JPL, NHSC. Support for this work was provided by NASA through an award issued by JPL/Caltech.

Facility: Herschel/HIFI

REFERENCES

Aalto, S., Garcia-Burillo, S., Muller, S., et al. 2012, A&A, 537, A44
Bolatto, A. D., Warren, S. R., Leroy, A. K., et al. 2013, Natur, 499, 450
Bradford, C. M., Stacey, G. J., Fischer, J., et al. 1999, in The Universe as Seen by ISO, ed. P. Cox & M. F. Kessler (ESA-SP 427; Noordwijk: ESA), 861
Brock, D., Joy, M., Lester, D. F., Harvey, P. M., & Ellis, H. B., Jr. 1988, ApJ, 329, 208
Chou, R. C., Peck, A. B., Boone, F., & Henkel, C. 2007, ApJ, 670, 116
Colbert, E. J. M., Baum, S. A., Gallimore, J. F., et al. 1996, ApJS, 105, 75
Dahlem, M., Golla, G., Whiteoak, J. B., et al. 1993, A&A, 270, 29
Davies, R. I., Maciejewski, W., Hicks, E. K. S., et al. 2009, ApJ, 702, 114
de Graauw, Th., Helmich, F. P., Phillips, T. G., et al. 2010, A&A, 518, L6
Emprechtinger, M., Monje, R. R., van der Tak, F. F. S., et al. 2012, ApJ, 756, 136
Forbes, D. A., Polehampton, E., Stevens, I. R., Brodie, J. P., & Ward, M. J. 2000, MNRAS, 312, 689
Franklin, J., Snell, R. L., Kaufman, M. J., et al. 2008, ApJ, 674, 1015
Gear, W. K., Gee, G., Rodson, E. I., et al. 1986, MNRAS, 219, 19
Henkel, C., Whiteoak, J. B., Nyman, L.-Å, & Harju, J. 1990, A&A, 230, L5
Karachentsev, I. D., Tully, R. B., Dolphin, A., et al. 2007, AJ, 133, 504
Kennicutt, R. C., Jr. 1998, ApJ, 498, 541
Koribalski, B., Whiteoak, J. B., & Houghton, S. 1995, PASA, 12, 20
Kristensen, J., Visser, R., van Dishoeck, E. F., et al. 2010, A&A, 521, L30
Krug, H. B., Rupke, D. S. N., & Veilleux, S. 2010, ApJ, 708, 1145
Lin, L.-H., Taam, R. E., Yen, D. C. C., Muller, S., & Lim, J. 2011, ApJ, 731, 11
Marconi, A., Oliva, E., van der Werf, P. P., et al. 2000, A&A, 357, 24
Melo, V. P., Pérez García, A. M., Acosta-Pulido, J. A., et al. 2002, ApJ, 574, 709
Monje, R. R., Emprechtinger, M., Phillips, T. G., et al. 2011a, ApJL, 734, L23
Monje, R. R., Phillips, T. G., Peng, R., et al. 2011b, ApJL, 742, L21
Müller-Sánchez, F., González-Martín, O., Fernández-Ontiveros, J. A., Acosta-Pulido, J. A., & Prieto, M. A. 2010, ApJ, 716, 1166
Murray, N., Quataert, E., & Thompson, A. 2005, ApJ, 618, 569
Neufeld, D. A., Sonnentrucker, P., Phillips, T. G., et al. 2010, A&A, 518, L108
Neufeld, D. A., Wolre, M. G., & Schilke, P. 2005, ApJ, 628, 260
Nolt, I. G., Radostitz, J. V., DiLonardo, G., et al. 1987, JMoSp, 125, 274
Ott, M., Whiteoak, J. B., Henkel, C., & Wielebinski, R. 2001, A&A, 372, 463
Ott, S. 2010, in ASP Conf. Ser. 434, Astronomical Data Analysis Software and Systems XIX, ed. Y. Mizumoto, K.-I. Morita, & M. Ohishi (San Francisco, CA: ASP), 139
Pettini, M., Shapley, A. E., Steidel, C. C., et al. 2001, ApJ, 554, 981
Phillips, T. G., Bergin, E. A., Lis, D. C., et al. 2010, A&A, 518, L109
Pilbratt, G. L., Riedinger, J. R., Passvogel, T., et al. 2010, A&A, 518, L1
Radovich, M., Kahanpäa, J., & Lemke, D. 2001, A&A, 377, 73
Rangwala, N., Maloney, P. R., Glenn, J., et al. 2011, ApJ, 743, 94
Roelfsema, P. R., Helmich, F. P., Teyssier, D., et al. 2012, A&A, 537, A17
Rupke, D. S., Veilleux, S., & Sanders, D. B. 2005, ApJS, 160, 87
Silk, J., & Rees, M. J. 1998, A&A, 331, L1
Sonnentrucker, P., Neufeld, D. A., Phillips, T. G., et al. 2010, A&A, 521, L12
Strickland, D. K., Heckman, T. M., Colbert, E. J. M., Hoopes, C. G., & Weaver, K. A. 2004, ApJ, 606, 829
Strickland, D. K., Heckman, T. M., Weaver, K. A., & Dahlem, M. 2000, AJ, 120, 2965
Sturm, E., González-Alfonso, E., Veilleux, S., et al. 2011, ApJL, 733, L16
Turner, B. E. 1985, ApJ, 299, 312
Van der Tak, F. F. S., Ossenkopf, V., Nagy, Z., et al. 2012, A&A, 537, L10
Van der Werf, P. P., Isaak, K. G., Meijerink, R., et al. 2010, A&A, 518, L42
Veilleux, S., Cecil, G., & Bland-Hawthorn, J. 2005, ARA&A, 43, 769
Weaver, K. A., Heckman, T. M., Strickland, D. K., & Dahlem, M. 2002, ApJL, 576, L19
Westmoquette, M. S., Smith, L. J., & Gallagher, J. S., III. 2011, MNRAS, 414, 3719
Whiteoak, J. B., Dahlem, M., Wielebinski, R., & Harnett, J. I. 1990, A&A, 231, 25
Whiteoak, J. B., & Wilson, W. E. 1990, MNRAS, 245, 665
Young, J. S., Xie, S., Tacconi, L., et al. 1995, ApJS, 98, 219